THE IMPACT OF UVCS/SOHO OBSERVATIONS ON MODELS OF ION-CYCLOTRON RESONANCE HEATING OF THE SOLAR CORONA

S. R. Cranmer[1], G. B. Field[1], G. Noci[2], and J. L. Kohl[1]

[1]Smithsonian Astrophysical Observatory, Cambridge, MA 02138, USA
[2]Università di Firenze, I-50125 Firenze, Italy

ABSTRACT

We examine the compatibility between theoretical models and observations of the temperatures and anisotropic velocity distributions of hydrogen and minor ions in the solar corona. The UVCS instrument on board SOHO has measured hydrogen kinetic temperatures along lines of sight in coronal holes in excess of 3×10^6 K, and O^{+5} ion kinetic temperatures of at least 2×10^8 K. In addition, the velocity distributions in the radial direction (mainly perpendicular to the line of sight) are smaller, possibly implying temperature anisotropies of order $T_\perp / T_\parallel \approx 100$ for the oxygen ions.

These properties can only be understood in terms of a mechanism which heats and accelerates heavier ions more than lighter ones (possibly proportionally to the ion mass to a power higher than unity), and preferentially in directions perpendicular to the magnetic field. We examine various features of plasma heating by the dissipation of high-frequency ion-cyclotron resonance Alfvén waves, which may be the most natural physical mechanism to produce such plasma conditions. We present preliminary quantitative models of the ion motions in polar coronal holes, and show that such models can be used to predict the spectrum of waves required to reproduce the observations. Indeed, the more ionic species that are observed spectroscopically, the greater the extent in frequency space the wave spectrum can be inferred.

Key words: solar corona; solar wind; plasma physics.

1. INTRODUCTION

In order to better understand the mechanisms which heat and accelerate the solar wind, theories must incorporate empirical measurements of the physical conditions of coronal plasma. Ultraviolet spectroscopy of the hot and highly-ionized inner corona is especially suited to help determine densities, temperatures, and velocity distributions in the region of the solar wind where most of the momentum and energy is deposited (see reviews by Withbroe et al. 1982; Bely-Dubau 1994). In this presentation we utilize recent results from the *Ultraviolet Coronagraph Spectrometer* (UVCS), operating aboard the *Solar and Heliospheric Observatory* (SOHO) satellite, to constrain theoretical models of the fast solar wind.

In Section 2 we summarize the results of an empirical model for the plasma parameters of the O^{+5} ion which has been constructed from UVCS observations at solar minimum (Kohl et al. 1998). In the open-field regions of the solar wind, we infer extremely strong temperature anisotropies for O^{+5}, with microscopic velocities perpendicular to the field lines of order 600 km s^{-1}. In Section 3 we discuss a scenario for heating and accelerating minor ions to observed temperatures and velocities via the dissipation of high-frequency Alfvén waves in resonance with the cyclotron gyrofrequencies of individual particles. In Section 4 we present a preliminary kinetic model of the radial and perpendicular motion of a representative ion in the presence of ion-cyclotron heating, and show that temperature anisotropies and high-speed wind acceleration are a natural result of the assumed wave dissipation mechanism. In Section 5 we briefly discuss the implications of these results on more comprehensive solar wind models, and outline directions for future work.

2. EMPIRICAL MODEL OF CORONAL HOLES

The UVCS instrument is described in detail by Kohl et al. (1995), and some preliminary first results have been presented by Kohl et al. (1996, 1997a, 1997b) and Noci et al. (1997). The UVCS telescope spectrometer unit contains three independent channels: (1) the LYA (Lyman α) toric grating spectrometer, which primarily observes the strong H I λ1216 emission line, (2) the OVI toric grating spectrometer, which is optimized to observe the O VI $\lambda\lambda$1032, 1037 doublet and the H I λ1026 (Lyman β) line, and (3) the WLC (white light channel) visible polarimeter, which measures the coronal polarized radiance in the 4500–6000 Å wavelength band. At least 31 different UV spectral lines have been identified in the solar corona by UVCS during its first year of operation (Raymond et al. 1997).

In this presentation we utilize results from the empirical model of Kohl et al. (1998), which collected a

large ensemble of UVCS observations from the period between November 1996 and April 1997, and presented self-consistent 3D distributions of density, velocity, kinetic temperature, and abundance for electrons, neutral hydrogen, and O^{+5} ions in open-field coronal hole regions. We discuss mainly the plasma kinetic properties of the minor ion O^{+5} inferred from the intensities and line-shapes of the O VI $\lambda\lambda$1032, 1037 doublet.

The most surprising initial results from the first year of operation of UVCS have been the extremely broad profiles of these emission lines (see Figure 1). Their Doppler widths probe the microscopic velocity distribution along the observational line of sight (LOS). Kohl et al. (1997a) found that O VI emission lines over polar coronal holes are well-fit by single Gaussian functions, implying largely Maxwellian distributions along this direction. For observations off the limb, the region along the LOS with strongest contribution to line emissivity lies *perpendicular* to the nearly-radial magnetic field.

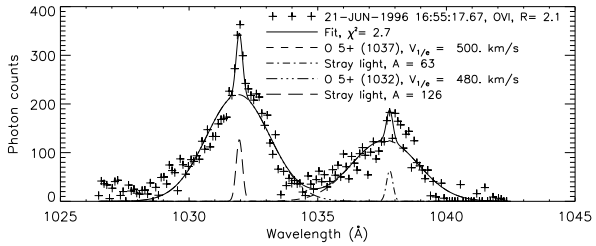

Figure 1. Example O VI line profiles in the north polar coronal hole, centered at a heliocentric height of 2.1 $R_\odot$. Constrained nonlinear least-squares fits were used to account for the contribution from instrumental stray light and the F corona. See Kohl et al. (1997a) for details.

In Figure 2 we plot the $1/e$ half-widths of both components of the O VI doublet, expressed in Doppler velocity units (see Kohl et al. 1998). Measurements from the 1032 line are plotted with squares and triangles, and measurements from the 1037 line are plotted with diamonds and crosses; we find no systematic differences between the two components. The velocities inferred from the broad O VI lines are extremely large compared to those assuming thermal equilibrium with the electrons (dotted line). The electron temperatures assumed here have been derived from *in situ* charge state measurements made by the SWICS instrument on *Ulysses* (Ko et al. 1997).

The Doppler widths of the bright Lyα emission line in coronal holes are significantly smaller than those of the O VI lines. From 2 to 4 $R_\odot$ from sun-center, the $1/e$ half-width of Lyα slowly increases by about 50 km s^{-1}, from $\sim$ 200 to 250 km s^{-1} (Kohl et al. 1998). As can be seen in Figure 2, however, the shapes of the O VI $\lambda\lambda$1032, 1037 lines grow much broader over this range of radii, by about 300 km s^{-1}. Converted into "kinetic temperature" T_K by $V_{1/e} = (2kT_K/m_{\rm ion})^{1/2}$, the line-widths imply strong deviations from thermal equilibrium: at a fiducial radius of 3 $R_\odot$, $T_K \approx 3.5 \times 10^6$ K for neutral hydrogen atoms, and $T_K \approx 200 \times 10^6$ K for O^{+5} ions.

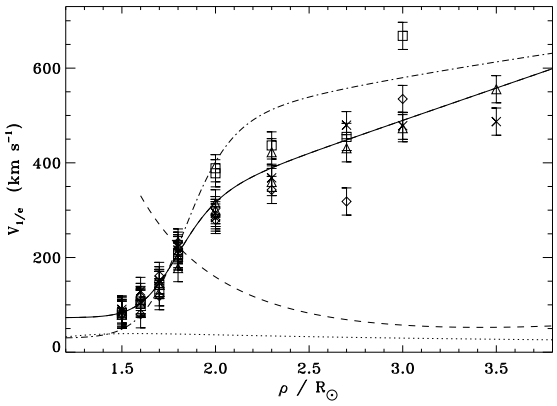

*Figure 2. Measured $V_{1/e}$ line-widths (*points*), and best fit to data (*solid line*). Also: microscopic speed $w_e = (2kT_e/m_{\rm ion})^{1/2}$ (*dotted line*), maximum allowed parallel O VI microscopic speed from line-ratio constraints (*dashed line*), and modeled $w_\perp$ velocity (*dot-dashed line*).*

Further empirical information about the O^{+5} ions has been extracted from the ratio of total intensities between the two lines of the doublet. This is primarily done by modeling the "Doppler dimming" effect, determined by the amount of Doppler shift between the incident solar-disk intensity profiles and the moving coronal gas (Hyder & Lites 1970; Beckers & Chipman 1974; Kohl & Withbroe 1982; Strachan et al. 1993). Specifically, Noci, Kohl, & Withbroe (1987) found that the ratio for these lines is a sensitive probe of both the bulk outflow velocity and the radial (i.e., *parallel*) microscopic velocity distribution.

Because of "pumping" by a nearby C II λ1037 line, the O VI line ratio can be used to put a firm upper limit on the radial $1/e$ microscopic speed (dashed line in Figure 2), which for most radii lies well below the observed speeds in the perpendicular direction. This is unambiguous evidence that $T_\perp > T_\parallel$ for O^{+5} ions in the extended corona. The self-consistent empirical model constructed by Kohl et al. (1998) also exhibited a "true" perpendicular speed (dot-dashed line) slightly larger than the observed line-width velocity because of LOS-integration effects.

Although the line ratio provides an upper limit on the parallel microscopic speed of O^{+5} ions, the only plausible lower limit comes from assuming equal temperatures (in this direction only) with electrons. Using these two limits, Kohl et al. (1998) computed the magnitude of the ion outflow velocity that is consistent with the observations, and these are plotted in Figure 3. These velocities are of the same order as the inferred proton-electron flow speeds computed from mass flux conservation.

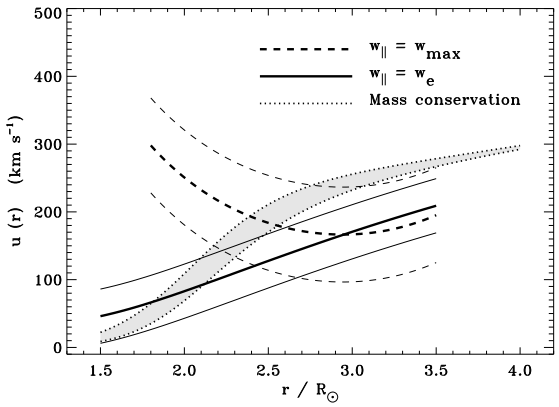

Figure 3. Modeled O^{+5} outflow velocity over the poles. Solid and dashed lines denote two models with lower and upper limits for $w_\parallel$. Error bars are derived from uncertainties in modeled n_e, T_e, and chromospheric intensity. The shaded region represents proton mass flux conservation with Kopp & Holzer (1976) divergence factors $f_{\max} = 6.5$ (upper dotted line), and $f = 1$ (lower dotted line).

3. ION-CYCLOTRON RESONANCE DISSIPATION

3.1. Motivation

It has been known for several decades that minor ions in the solar wind have anisotropic velocity distributions and are accelerated to approximately the same outflow speed as the protons, but the measurements described above extend this knowledge down into the subsonic acceleration region of the wind. In addition, the observed microscopic speeds of minor ions such as O^{+5} are significantly larger than those observed for neutral hydrogen and protons, implying that neither thermal (common-temperature) Doppler motions nor bulk MHD motions (e.g., waves or turbulence) along the LOS are the dominant line-broadening mechanisms. Some additional perpendicular energy deposition is required which preferentially broadens the velocity distributions of the heavier ions, with the resulting kinetic temperatures proportional to the ion mass to a power higher than unity. Indeed, there is preliminary evidence from UVCS/SOHO to suggest that this phenomenon extends up to the Mg^{+9} and Si^{+12} ions as well (Kohl et al. 1997a).

A probable theoretical explanation for many features of the preferential ion heating is high-frequency wave dissipation via resonance with ion-cyclotron Larmor motions about the coronal magnetic field lines (see, e.g., Isenberg & Hollweg 1983; Isenberg 1984; McKenzie, Banaszkiewicz, & Axford 1995; Tu & Marsch 1997). Wave-particle interactions of this kind in the solar wind have been suspected since *in situ* measurements have shown that most heavy ions flow slightly faster than protons, with differential speeds of the same order as the Alfvén speed (Marsch et al. 1981).

3.2. Mechanism

Magnetohydrodynamic (MHD) waves are an important component of the solar wind. It is commonly assumed that, of the several varieties of MHD waves, only the incompressible transverse Alfvén modes can propagate relatively unattenuated into the solar wind (see, e.g., Khabibrakhmanov & Summers 1997). Let us then examine the effects of these oscillations on solar-wind momentum and energy conservation.

Small-amplitude (first-order) Alfvén waves induce local variations in the perpendicular electromagnetic fields $\mathbf{E}_\perp$ and $\mathbf{B}_\perp$ and in the transverse velocities $\mathbf{u}_\perp$ of different particle species. The fluid momentum balance is affected via the Lorentz force and "centrifugal" effects of gyrating particle velocities. First-order terms average to zero over a wave period, and second-order terms provide a net acceleration:

$$\mathbf{a}_w = \frac{q}{mc} \langle \mathbf{u}_\perp \times \mathbf{B}_\perp \rangle + \frac{\langle |\mathbf{u}_\perp|^2 \rangle}{r} \quad , \qquad (1)$$

where we assume the waves are propagating parallel to the radial zero-order field ($\mathbf{k} \parallel \mathbf{B}_r$). Correspondingly, second-order Joule dissipation does work on the particles and results in a volumetric heating term in the energy conservation equation:

$$Q_w = \frac{q}{m} \langle \mathbf{u}_\perp \cdot \mathbf{E}_\perp \rangle \quad , \qquad (2)$$

which is intimately related to the acceleration terms in the momentum equation (Isenberg & Hollweg 1982).

The standard "wave pressure" formalism for evaluating these quantities deals mainly with large-scale radial gradients in the fields and fluctuation velocities. It also neglects the substantial resonance effects which occur when the comoving wave frequency $(\omega - u_\parallel k)$ approaches the local Larmor ion-cyclotron frequency $\Omega \equiv qB_r/mc$. Note that this frequency is proportional to the ion charge-to-mass ratio Z/A, which is less than one for all elements in all stages of ionization other than H^+. Because the cyclotron frequency depends on the radial magnetic field strength, it decreases monotonically with increasing radius. Thus, at different radii, different waves will be in resonance with the local Ω.

Near the ion-cyclotron resonance, the coupling between particle and wave motions becomes increasingly strong, and it is sensitive to the shape of the microscopic velocity distribution. As in Landau damping, the pitch-angle dependence of the distribution determines whether particles gain or lose energy at the expense of the waves (see, e.g., Benz 1993). Heuristically, this damping produces a small imaginary part of the wavenumber k, causing an added *real* acceleration when taking the gradient of e^{ikr} wave terms.

McKenzie & Marsch (1982) evaluated these added acceleration and heating terms, and found that for realistic bi-Maxwellian distributions the ion-cyclotron resonance (for left-polarized waves) indeed dissipates the waves and accelerates and heats the ions:

$$a_{w,r}^{\rm res} \approx \frac{\Omega^3}{w_\parallel k^2} \frac{B_\perp^2}{B_r^2} \exp\left[- \left(\frac{\omega - u_\parallel k - \Omega}{w_\parallel k} \right)^2 \right] \qquad (3)$$

$$Q_w^{\rm res} \approx \frac{\omega}{k}\, a_{w,r}^{\rm res} \ , \qquad (4)$$

where $w_\parallel$ is the parallel $1/e$ microscopic speed of the bi-Maxwellian distribution. Note that the resonance condition in the exponential effectively filters out wave frequencies far from Ω. This dissipation results in a temporal rate of change of an individual particle's kinetic energy of order $\Omega(m|\mathbf{u}_\perp|^2/2)$. The efficiency of this process results from the fact that the energy is damped out on an extremely rapid time scale ($\Omega^{-1} \approx 10^{-3}$ s).

The magnitudes of the resonant acceleration/heating terms are approximately $\mathcal{O}(kr) \approx 10^5$–$10^7$ times larger than the corresponding nonresonant terms, assuming equal wave amplitudes in all frequency regimes. Thus, even if the power in the high-frequency (50–5000 Hz) near-resonant wave spectrum is several orders of magnitude smaller than the power at more conventional low frequencies (0.01–1 Hz), the resonant terms described above may still dominate the solar-wind momentum and energy balance.

4. A SIMPLE KINETIC MODEL

To show how resonant wave heating can produce hot and anisotropic ion motions, we model the collisionless corona by following the motion of individual particles. A charged particle moving in a spatially-varying magnetic field experiences a "magnetic-mirror" force proportional to its magnetic moment (Spitzer 1962), and we can write the radial equation of motion as

$$m\frac{dv_r}{dt} = \frac{dE_\parallel}{dr} = -\mu\frac{dB_r}{dr} - mg_{\rm eff} \qquad (5)$$

where $E_\parallel$ is the kinetic energy in the radial direction, $\mu = E_\perp/B$ is the magnetic moment, and $g_{\rm eff}$ represents the net effective gravity, slightly modified by a zero-current electrostatic field. (The magnetic mirror term above corrects an error in the corresponding equation in Cranmer, Field, & Kohl 1997.)

We address the dissipation of Alfvén waves by assuming that the heating described above dominates the net rate of change of the total particle kinetic energy:

$$v_r\frac{d}{dr}\left(E_\parallel + E_\perp\right) = mQ_w^{\rm res} \ , \qquad (6)$$

where $Q_w^{\rm res}$ is evaluated exactly at resonance with the oxygen ions. Equations (5) and (6) are two ordinary differential equations in two unknowns, $E_\parallel$ and $E_\perp$, and can be integrated in radius from a specified initial condition. Note that this formulation naturally provides the linkage between the heating and the acceleration (in the magnetic mirror term) that was implied above.

Figure 4 shows the result of numerically integrating these equations for a representative O^{+5} ion starting at $r = 1.75R_\odot$, near the point where empirical models indicate these ions become collisionless (Kohl et al. 1998). A power spectrum of wave frequencies is assumed ($P \propto \omega^{-1}$), with the radial evolution of the velocity amplitude determined by conservation of wave action (Khabibrakhmanov & Summers 1997). The densities and bulk outflow speeds for the background proton-electron wind are specified by the UVCS empirical model (Kohl et al. 1998). At resonant frequencies, only small wave amplitudes are required to produce significant heating ($u_\perp \approx 0.1$ km s^{-1}).

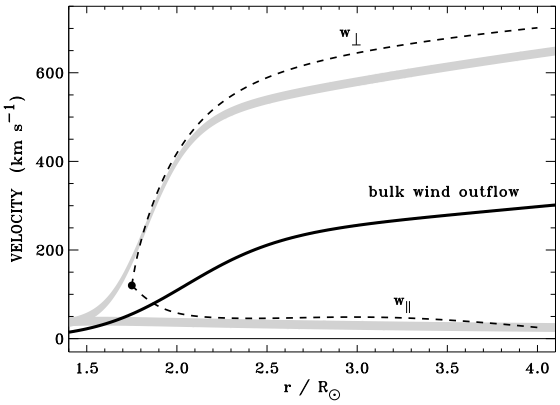

*Figure 4. Numerical O^{+5} velocities $w_\perp = v_\perp$ and $w_\parallel = v_r - u_\parallel$ for the collisionless wind model (*dashed lines*). Also plotted is $u_\parallel$ (*solid line*) from mass flux conservation, and the empirical perpendicular and parallel microscopic speeds from Figures 2 and 3 (*gray regions*).*

The representative ion gains kinetic energy in all directions, and we interpret its *perpendicular* velocity as being characteristic of the $1/e$ microscopic speed of ions in a distribution. Its *parallel* velocity v_r, however, can be interpreted as either bulk outflow or a corresponding parallel "thermal speed." In Figure 4 we decompose v_r into a simple sum of these two components; note that v_r itself does increase with radius, implying net outward particle acceleration. The decomposition of v_r into $(u_\parallel + w_\parallel)$, however assumes the particle always remains a representative member of its local velocity distribution. This remains to be verified with full calculations of the distribution function (either with, e.g., the BGK Boltzmann equation or with Monte Carlo simulations) and we anticipate the results to not vary significantly from this single-particle evolution. In such calculations, though, collisions must then be taken into account, because a small amount dynamical friction is required to maintain the nearly-isotropic cores of even the most anisotropic distributions (e.g., Livi & Marsch 1987). This work is ongoing.

5. RESULTS AND CONCLUSIONS

The UVCS/SOHO empirical measurements described in this paper have shown that the solar wind arising from coronal holes begins to behave as a nonequilibrium collisionless plasma by $r \approx 2$–$3R_\odot$. It is necessary to consider heating and acceleration mechanisms which act preferentially toward heavy ions and produce perpendicular temperatures which scale as the ion mass to a power higher than unity. The dissipation of ion-cyclotron resonance Alfvén

waves is a feasible way of producing this energy and momentum deposition.

Because different ions have different resonant frequencies, they receive different amounts of heating and acceleration as a function of radius. *Thus, the more species are observed, the greater range of wave frequencies that can be probed.* Also, because minor ions such as O^{+5} represent a negligible fraction of the total solar-wind number density, their absorption of wave energy should not appreciably alter the outgoing wave train. This fact can be used to probe the same waves at different radii, as they resonate with ions with progressively larger Z/A until they are finally damped out by the proton resonance in the outer corona.

The precise mechanisms for generating the required high frequencies (50–5000 Hz) are currently unclear. Isenberg & Hollweg (1983) proposed and developed the scenario of Alfvén-wave saturation followed by turbulent cascade from low to high frequencies. Alternately, Axford & McKenzie (1991) suggested that reconnections in small (< 100 km) closed-loop "micro-flares," distributed finely through the chromospheric network, are able to generate high-frequency waves that can propagate outwards into the corona. There seems to be no theoretical limitation on extending observed MHD turbulence and magnetic reconnection activity down below the smallest resolvable scales.

It is possible that the TRACE (Transition Region and Coronal Explorer; Strong et al. 1994) instrument may be able to better distinguish between the several viable scenarios by obtaining precisely coaligned, high-resolution, and high-cadence image sequences in the photosphere, transition region, and corona. Current measurements of the statistical energy spectrum of micro-flare events are unclear as to whether the smallest-scale structures play a significant role in coronal heating and acceleration (Porter et al. 1995; Shimizu & Tsuneta 1997). MHD waves can be detected in coronal fine structures by observing either periodic intensity fluctuations or oscillatory motions of flux tubes; instruments like *Yohkoh* have already begun to measure such motions in various structures (e.g., McKenzie 1997).

In any case, it does now seem possible to construct self-consistent theories of coronal plasma heating that are constrained by coronagraphic observations of anisotropic ion velocity distributions. The ability of high-frequency waves to preferentially heat and accelerate heavy ions in high-speed wind streams is becoming very clear.

ACKNOWLEDGMENTS

This work is supported by the National Aeronautics and Space Administration under grant NAG5-3192 to the Smithsonian Astrophysical Observatory, by Agenzia Spaziale Italiana, and by Swiss funding agencies.

REFERENCES

Axford, W. I., & McKenzie, J. F. 1991, in Solar Wind Seven (COSPAR Coll. Ser. 3), 1

Beckers, J. M., & Chipman, E. 1974, Solar Phys., 34, 151

Bely-Dubau, F. 1994, Adv. Space Res., 14, no. 4, 153

Benz, A. O. 1993, Plasma Astrophysics: Kinetic Processes in Solar and Stellar Coronae (Dordrecht: Kluwer)

Cranmer, S. R., Field, G. B., & Kohl, J. L. 1997, in Tenth Cambridge Workshop on Cool Stars, Stellar Systems, and the Sun, in press

Hyder, C. L., & Lites, B. W. 1970, Solar Phys., 14, 147

Isenberg, P. A. 1984, J. Geophys. Res., 89, 6613

Isenberg, P. A., & Hollweg, J. V. 1982, J. Geophys. Res., 87, 5023

Isenberg, P. A., & Hollweg, J. V. 1983, J. Geophys. Res., 88, 3923

Khabibrakhmanov, I. K., & Summers, D. 1997, J. Geophys. Res., 102, 7095

Ko, Y.-K., Fisk, L. A., Geiss, J., Gloeckler, G., & Guhathakurta, M. 1997, Solar Phys., 171, 345

Kohl, J. L., et al. 1995, Solar Phys., 162, 313

Kohl, J. L., et al. 1996, Bull. AAS, 28, 897 (49.06)

Kohl, J. L., et al. 1997a, Solar Phys., in press

Kohl, J. L., et al. 1997b, Adv. Space Res., in press

Kohl, J. L., et al. 1998, ApJ, submitted

Kohl, J. L., & Withbroe, G. L. 1982, ApJ, 256, 263

Kopp, R. A., & Holzer, T. E. 1976, Solar Phys., 49, 43

Livi, S., & Marsch, E. 1987, J. Geophys. Res., 92, 7255

Marsch, E., Rosenbauer, H., Schwenn, R., Mühlhäuser, K.-H., & Denskat, K. U. 1981, J. Geophys. Res., 86, 9199

McKenzie, D. E. 1997, Publ. Astron. Soc. Pacific, 109, 739

McKenzie, J. F., Banaszkiewicz, M., & Axford, W. I. 1995, A&A, 303, L45

McKenzie, J. F., & Marsch, E. 1982, Astrophys. Space Sci., 81, 295

Noci, G., et al. 1997, Adv. Space Res., in press

Noci, G., Kohl, J. L., & Withbroe, G. L. 1987, ApJ, 315, 706

Porter, J. G., Fontenla, J. M., & Simnett, G. M. 1995, ApJ, 438, 472

Raymond, J. C., et al. 1997, Solar Phys., in press

Shimizu, T., & Tsuneta, S. 1997, ApJ, 486, 1045

Spitzer, L., Jr. 1962, Physics of Fully Ionized Gases, 2nd ed. (New York: Wiley)

Strachan, L., Kohl, J. L., Weiser, H., Withbroe, G. L., & Munro, R. H. 1993, ApJ, 412, 410

Strong, K., Bruner, M., Tarbell, T., Title, A., & Wolfson, C. J. 1994, Space Sci. Rev., 70, 119

Tu, C.-Y., & Marsch, E. 1997, Solar Phys., 171, 363

Withbroe, G. L., Kohl, J. L., Weiser, H., & Munro, R. H. 1982, Space Sci. Rev., 33, 17